JOURNAL OF VIROLOGY, Oct. 1976, p. 222-233

Vol. 20, No. 1
Printed in U.S.A.

Physical Maps for Herpes Simplex Virus Type 1 DNA for Restriction Endonucleases *Hind* III, *Hpa*-1, and *X. bad*

NEIL M. WILKIE

*Cold Spring Harbor Laboratory, Cold Spring Harbor, New York 11724, and Institute of Virology, Glasgow, G11 5JR Scotland**

Received for publication 10 May 1976

It has been proposed that the genome of herpes simplex virus type 1 (HSV-1) consists of two internal unique sequences, S and L, bounded by two sets of redundant sequences (P. Sheldrick and N. Berthelot, 1974). In this arrangement, terminal sequences (TR_S and TR_L) are repeated in an internal inverted form (IR_S and IR_L) and delimit S and L. Furthermore, a body of evidence has accumulated that suggests that S and L themselves are inverted, giving rise to four related forms of the HSV genome. In this study the ordering of restriction endonuclease fragments of HSV-1 DNA for physical maps has been studied using molecular hybridization techniques and the cleavage of isolated restriction endonuclease fragments with further restriction endonucleases. Physical maps for the fragments produced by *Hind* III, *Hpa*-1, and *X. bad* have been constructed for the four related forms of the HSV-1 genome. TR_S and IR_S were found to be between 3.5×10^6 and 4.5×10^6 daltons, TR_L and IR_L about 6×10^6 daltons, S about 8×10^6 to 9×10^6 daltons, and L about 6.8×10^6 daltons.

The genome of herpes simplex virus type 1 (HSV-1) consists of a linear duplex DNA molecule of about 100×10^6 daltons. A true terminal redundancy of about 0.5×10^6 daltons (2, 3) is contained in somewhat larger blocks of terminal sequences which Sheldrick and Berthelot (10) found to be repeated in internal, inverted forms. Two unique sequences (S = 10^7 daltons; L = 75×10^6 daltons) were found to be bounded by these inverted repetitions. It was proposed that S was bounded at the terminus by TR_S and internally by the same sequence inverted, IR_S. Similarly, L was bounded by TR_L and IR_L. Sheldrick and Berthelot (10) also proposed that the unique sequences S and L might become relatively inverted by recombination events (see Fig. 10).

Subsequent work by various laboratories provided clear evidence that this model, including the relative inversions in S and L, was substantially correct. Restriction endonuclease cleavage analysis showed that submolar bands present in digests of both HSV-1 and HSV-2 DNA could be accounted for by the Sheldrick and Berthelot model (1, 4, 5, 8, 11, 14). In digests with endonucleases which cleave only in S and L, two 0.5 M terminal fragments are generated from each end. Four 0.25 M fragments, which span the internal inverted redundant sequences, also arise. If it is assumed that TR_L/IR_L and TR_S/IR_S are not identical, then enzymes that cleave in S and L, but in only the TR_L/IR_L pair on the TR_S/IR_S pair, generate a molar end from that terminus in which the redundant sequence is cleaved. Two 0.5 M fragments from the other terminus and two internal 0.5 M fragments are also present (see Fig. 10). Direct analysis of the terminal fragments found in restriction endonuclease digests of HSV-1 DNA, combined with sequence homology studies, confirmed these hypotheses (15) and provided further evidence that TR_L/IR_L and TR_S/IR_S were not identical. Finally, the relative inversions of S and L in the four genome arrangements for HSV-1 were visualized directly in the electron microscope via both incomplete (5) and complete partial denaturation maps (Delius and Clements, in press). In the latter study, TR_L/IR_L and TR_S/IR_S had different partial denaturation profiles.

This report gives the order of *Hind* III, *Hpa*-1, and *X. bad* fragments in the four genome arrangements for HSV-1 DNA.

MATERIALS AND METHODS

Enzymes. Restriction endonucleases *Hind* III and *Hpa*-1 were prepared as described previously (9, 14). *X. bad*, an enzyme from *Xanthamonus badrii*, was the kind gift of S. Zain. DNA polymerase I was purchased from the Boehringer Mannheim Corp., and DNase I was from Worthington.

Nick translation. HSV-1 DNA was labeled with α-^{32}P-labeled deoxyribonucleotide triphosphates (specific activity approximately 100 Ci/mmol; New England Nuclear Corp.) essentially as described by

Maniatis et al. (7). Reaction mixtures contained, in a volume of 100 μl: 1 μg of purified HSV-1 DNA; 50 mM Tris-hydrochloride, pH 7.8; 5 μM $MgCl_2$; 1 mM dithiothreitol; 50 μg of bovine serum albumin per ml; 180 pmol of [α-^{32}P]dTTP, [α-^{32}P]dGTP, [α-^{32}P]-dCTP, and [α-^{32}P]dATP; 2 units of DNA polymerase I; 10^{-10} g of DNase I per ml. Incubation was at 16°C for 1 h. The DNA was then extracted with phenol and purified by gel filtration on Sephadex G-50.

The growth of virus and DNA, end-labeling studies on HSV-1 DNA, restriction endonuclease digestion, analysis and purification of DNA fragments, the Southern DNA-transfer technique (12), and hybridization methods were carried out as described in the previous paper (15).

RESULTS AND DISCUSSION

The cleavage patterns of HSV-1 strain 17 DNA for *Hind* III, *Hpa*-1, *X. bad,* and an *X. bad-Hpa*-1 double digest are shown in Fig. 1. The molarity of each submolar band is shown for the single digests. The molecular weights of the *Hind* III and *Hpa*-1 fragments have been published previously (15), and the *X. bad* digest is discussed below. The over-molar group of fragments previously designated *Hpa*-1 *o* (15) are shown below to be derived from two separable map locations, and this group has therefore been subdivided into *Hpa*-1 *o* and *Hpa*-1 *o'*.

Highly labeled HSV-1 DNA was needed for the studies discussed below, and ^{32}P-labeled DNA of high specific activity was obtained by nick translation as described under Materials and Methods. At the end of the reaction, DNA with a specific radioactivity of 3×10^7 cpm per μg appeared to be intact (in the sense of double-strand molecular weight) and could be digested with restriction endonucleases to give normal profiles. Figure 1b shows an autoradiograph of nick-translated HSV-1 DNA, cleaved with *Hpa*-1 and separated by electrophoresis on an agarose slab gel. The profile obtained appears identical to that obtained with the unlabeled DNA shown in Fig. 1a. The autoradiogram was used as a template to enable the DNA bands to be excised directly for subsequent purification. Figure 2 shows that when the purified fragments were analyzed by gel electrophoresis their mobility had not altered.

Analysis of *Hind* III/*Hpa*-1 double digests. To aid the construction of linkage groups for different restriction endonuclease fragments, a comprehensive description of the *Hind* III/*Hpa*-1 double digest was obtained. ^{32}P-labeled *Hpa*-1 fragments were isolated as described above and further cleaved with *Hind* III. The reciprocal experiment was also carried out. The analysis of the *Hind* III cleavage products of some *Hpa*-1 fragments is shown in Fig. 2. The molecular weights of the products were estimated by reference to the standard cleavage products of HSV-1 DNA run on the outside slots of the slab gel.

The results of several experiments are summarized in Fig. 3. Each fragment present in the *Hind* III/*Hpa*-1 double digest was shown to derive from the indicated *Hind* III and *Hpa*-1 fragments by further cleavage. *Hind* III or *Hpa*-1 fragments present as limit fragments in the double digest (fragments not further cleaved by the alternative enzyme) are indicated. The terminal fragments in the double digest were located by end-labeling studies similar to those described in the previous paper (15), and their positions in single and double digests are indicated.

Sequence homology between fragments. The assignment of different restriction endonuclease fragments to linkage groups can also be deduced from sequence homology studies. ^{32}P-labeled *Hpa*-1 fragments were hybridized to unlabeled *Hind* III fragments (and vice versa) by using the DNA transfer or blot technique developed by Southern (12) and described in our previous publication (15). Some cross-hybridization results are presented in Fig. 4. It is evident from this figure that fragments which appeared to be fairly pure on the basis of their relative mobilities upon gel electrophoresis (Fig. 2) are, in fact, contaminated by sequences from many different regions of the genome. This contamination can also be seen in the further cleavage analysis of some isolated bands shown in Fig. 2. This problem of sequence contamination was also observed when DNA labeled in vivo was used, and it seems more likely to be an artifact due to the purification and separation methods used rather than to the method of labeling. The contaminating sequences in the ^{32}P-labeled *Hpa*-1 fragments cause hybridization to most *Hind* III fragments at levels above background. Nevertheless, the hybridization of the main *Hpa*-1 fragment in any reaction can readily be distinguished as more intense bands of radioactivity on the autoradiographs. The data presented in Fig. 5 and 6 summarize the data obtained in several such experiments in which ^{32}P-labeled *Hind* III fragments were annealed to unlabeled *Hpa*-1 fragments and vice versa.

Construction of a partial map. In the previous publication (15) the four terminal fragments in *Hind* III digests of HSV-1 DNA were identified as *Hind* III *d, g,* and *m* and either *h* or *i* (not separated by the gel electrophoresis). *Hind* III *i* is arbitrarily designated as the terminal 0.5 M band. In *Hpa*-1 digests, the three terminal fragments were identified as a molar

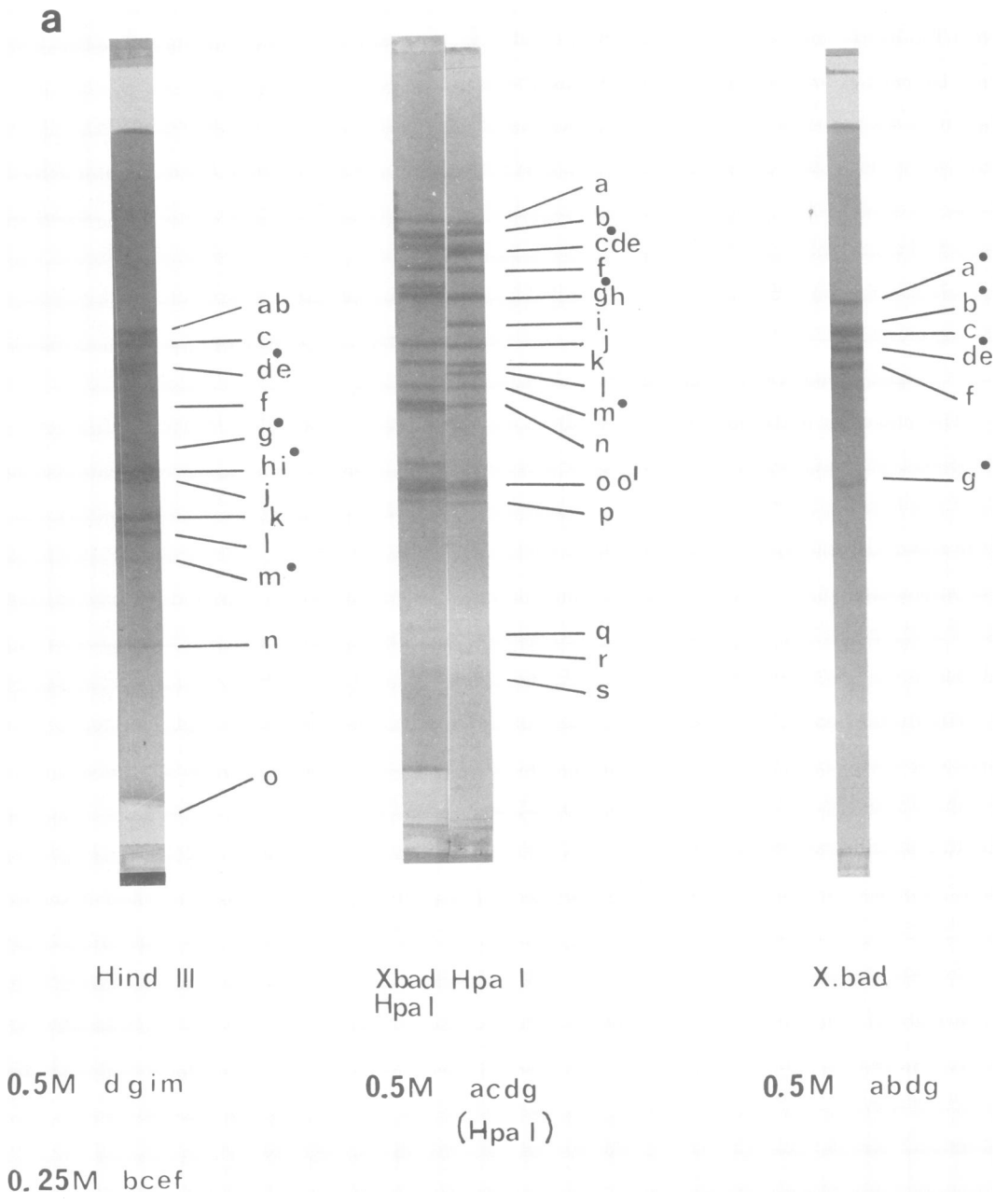

FIG. 1. *(a) Restriction endonuclease profiles of HSV-1 DNA. About 1 μg of HSV-1 DNA was cleaved with the restriction endonucleases shown and separated by electrophoresis on 0.3% agarose. Each fragment was assigned a letter of the alphabet. Hpa-1 o', an over-molar group of fragments, has been subdivided into two classes, o and o', for reasons explained in the text. Minor bands of molarities 0.25 or 0.5 are indicated. Terminal fragments are indicated by the solid circle (●). (b) The profile of nick-translated HSV-1 DNA. ^{32}P-labeled nick-translated DNA was cleaved with Hpa-1 and separated by electrophoresis on a slab gel of 0.7% agarose.*

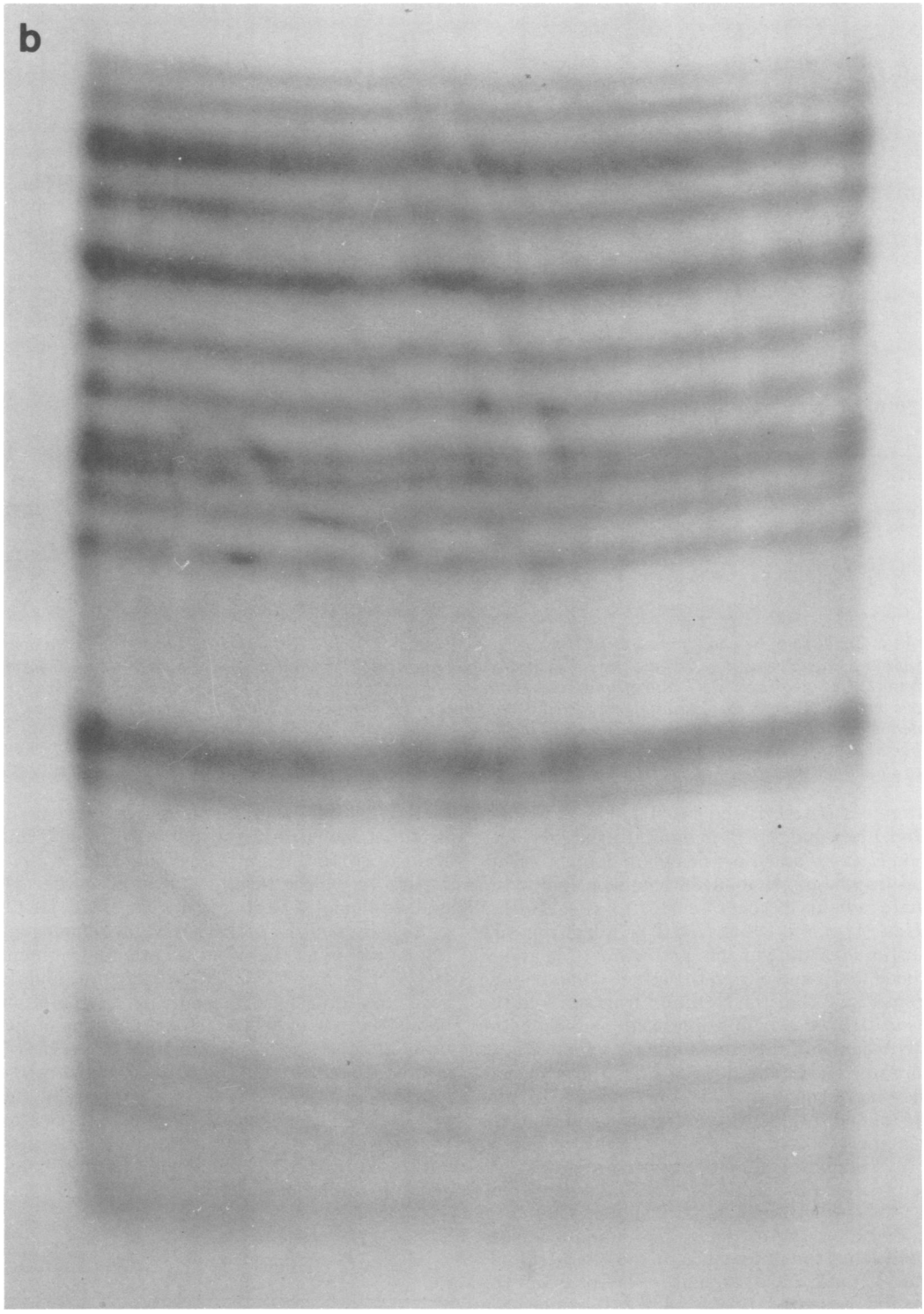
b

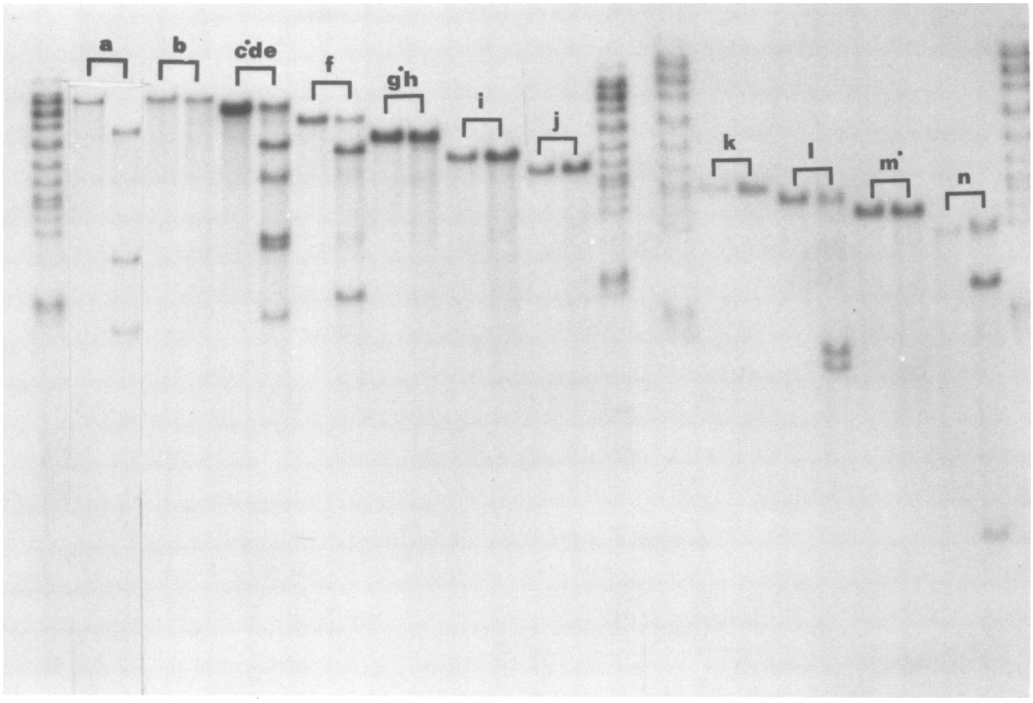

FIG. 2. *Further cleavage products of Hpa-1 fragments with Hind III.* ^{32}*P-labeled Hpa-1 fragments were isolated as described.* 2×10^3 *to* 2×10^4 *cpm of each fragment (less than 1 p) was mixed with 0.5 μg of unlabeled adenovirus-2 DNA and cleaved with Hind III. The cleaved fragments were separated by electrophoresis on slab gels of 0.7% agarose. Undigested fragments were run in parallel slots. In each case the unlabeled adenovirus-2 DNA was digested to limit products as determined by DNA-ethidium bromide fluorography. Labeled DNA was determined by autoradiography. Standard Hpa-1 cleavage products of total HSV-1 DNA are shown on the outside slots. Hpa-1 fragments from the termini are indicated by the solid circle (●).*

fragment *Hpa*-1 *m* and two 0.5 M fragments in *Hpa*-1 *cde* and *hg*. By a similar arbitrary decision *Hpa*-1 *d* and *g* are designated as the terminal fragments. Evidence was also presented in the previous publication (15) to suggest that *Hind* III *d* and *i* and *Hpa*-1 *m* were from one terminus of the genome and *Hind* III *g* and *m* and *Hpa*-1 *c* and *g* from the other. It can be seen from Fig. 3 that the terminal fragments in the *Hind* III/*Hpa*-1 double digests all arise from the DNA bands of the single digests which are, or contain, ends. The data of Fig. 3 are in complete agreement with the previous assignment (15) of end fragments to different termini of the genome.

By combining this information and the data summarized in Fig. 3, 5, and 6, a partial map for the *Hind* III and *Hpa*-1 fragments has been constructed. For example, Fig. 5 and 6 demonstrate that the unique fragments *Hind* III *j* and *Hpa*-1 *j* and *n* are sequence related. From the results presented in Fig. 2 and 3, it can be seen that there is a *Hpa*-1 site in *Hind* III *j* and a *Hind* III site in *Hpa*-1 *n*, but no *Hind* III site in *Hpa*-1 *j*. Furthermore, *Hpa*-1 *n* and *Hind* III *j* give rise to the same double-digest fragment "*o*." The molecular weights of the further cleavage products (not shown) suggest that at one end of this linkage group there must be *Hind* III and *Hpa*-1 sites very close together. The only other sequence homology for *Hpa*-1 *n* in *Hind* III digests is in *Hind* III *ab* (Fig. 6). The homologous sequences must lie in the unique fragment *Hind* III *a*, since *b* is a 0.25 M fragment, and its sequences must be present in other minor bands because of the relative inversions of the unique sequences S and L in HSV DNA. *Hpa*-1 *n* must therefore span the *Hind* III *a*-*Hind* III *j* junction. Analogous reductive analysis of the results shown in Fig. 3, 5, and 6 indicates that *Hpa*-1 *b, h, i,* and *q* must be contained within *Hind* III *a*. The following large linkage group is thus constructed:

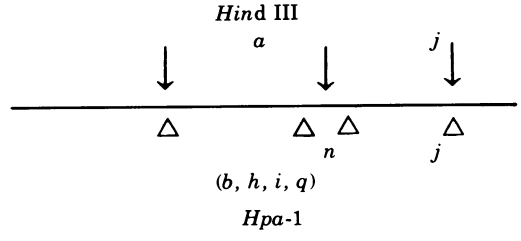

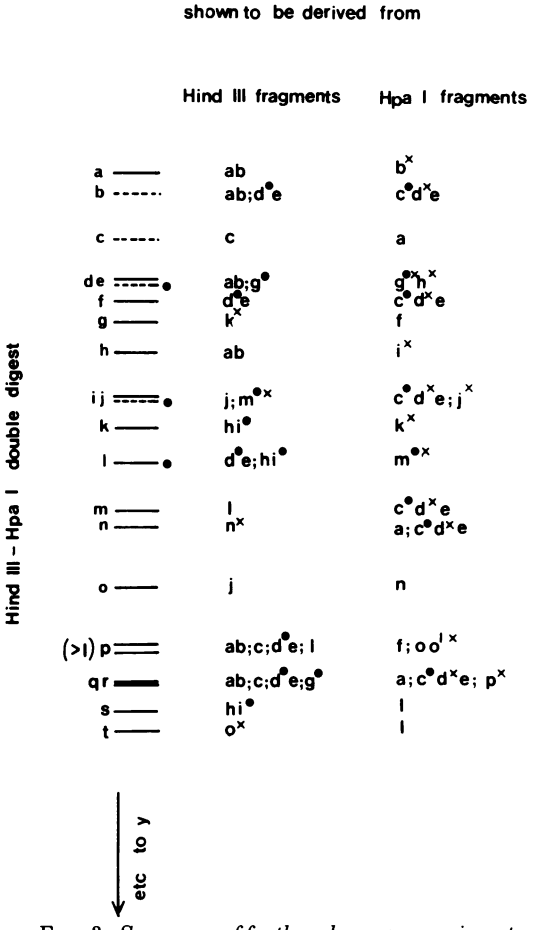

FIG. 3. *Summary of further cleavage experiments. On the basis of further cleavage experiments, bands of DNA in Hpa-1/Hind III double digests were shown experimentally to have arisen from the cleavage of Hind III fragments with Hpa-1 and of Hpa-1 fragments with Hind III. Solid circles (●) indicate fragments arising from termini. Crosses (X) indicate fragments of single digests which are not cleaved by the second enzyme and which exist as limit fragments in the double digest. For example, double-digest band k arises from the Hpa-1 cleavage of Hind III hi. Since Hpa-1 k is not further cleaved with Hind III, double-digest band k and Hpa-1 k must be identical. Hind III i is a terminal fragment. Hpa-1 k must therefore be contained within either Hind III h or Hind III i.*

Space does not permit a full analysis of the construction of all the linkage groups here. However, the data presented in Fig. 4, 5, and 6 contain all the information necessary to construct the partial map shown in Fig. 7. The linkage group containing *Hind* III *a* and *j* and that containing *Hind* III *h* could not be assigned map positions on the basis of the experiments with *Hind* III and *Hpa*-1 described so far. The limits of the map terminate at positions where the *Hind* III and *Hpa*-1 sites are so close together that no more overlaps could be obtained.

The tendency for *Hind* III *c* and *de* to anneal to *Hpa*-1 *b* is not accounted for in this partial map. Since further mapping data below puts *Hpa*-1 *b* firmly within *Hind* III *a*, it is thought that this aberrant annealing data is due to *Hind* III *a* sequences contaminating *Hind* III *c* and *de*.

The cleavage pattern for *Hpa*-1 arises from *Hpa*-1 sites in S and L and in either TR_S/IR_S or in TR_L/IR_L (1, 15). Therefore, one terminal fragment must be present in molar amounts. *Hpa*-1 *m* has been identified as a terminal fragment (15), but was originally quantified as 0.77 M and was thought to be a 0.5 M band (*Hpa*-1 *l* in reference 1). From the results presented here it is clear that *Hpa*-1 *m* arises from a cleavage within TR_L and must be the molar end. The reason for the apparently low amount of this terminal fragment in digests is not completely understood. We have noted that in many cases terminal fragments from both termini are more spread after gel electrophoresis than other bands of DNA (N. M. Wilkie, J. B. Clements, and R. Cortini, unpublished observations) as though there was some heterogeneity in their molecular weights. Such heterogeneity and spreading tends to reduce the peak height of the bands and in some cases may lead to a reduction in the observed amount of DNA in the bands. The reasons for the heterogeneity in terminal fragments remains a matter for speculation.

The hybridization and further cleavage experiments also confirm the general model for HSV DNA first proposed by Sheldrick and Berthelot (10). Bands of DNA containing submolar fragments from one enzyme digest cross-hybridize to the expected submolar fragments produced by the second enzyme. For example, *Hpa*-1 *a* (0.5 M) anneals to all of the submolar fragments in the *Hind* III digest (Fig. 4, 6). The terminal *Hpa*-1 fragment *m* hybridizes to the 0.25 M *Hind* III fragments and to the two *Hind* III terminal fragments *d* and *i*, but it does not anneal significantly to the *Hind* III terminal fragments *g* and *m*. This confirms the assignment of *Hpa*-1 *m* to the same terminus from which *Hind* III *d* and *i* arise. It might have been expected that the actual terminal redundancy of about 0.5×10^6 daltons previously proposed by other groups (2, 3, 10) might have caused some cross-hybridization between terminal fragments from different ends of the genome. However, the nearby inverted repeat of the terminal sequences found in HSV-1 DNA by Hyman et al. (6) and subsequently con-

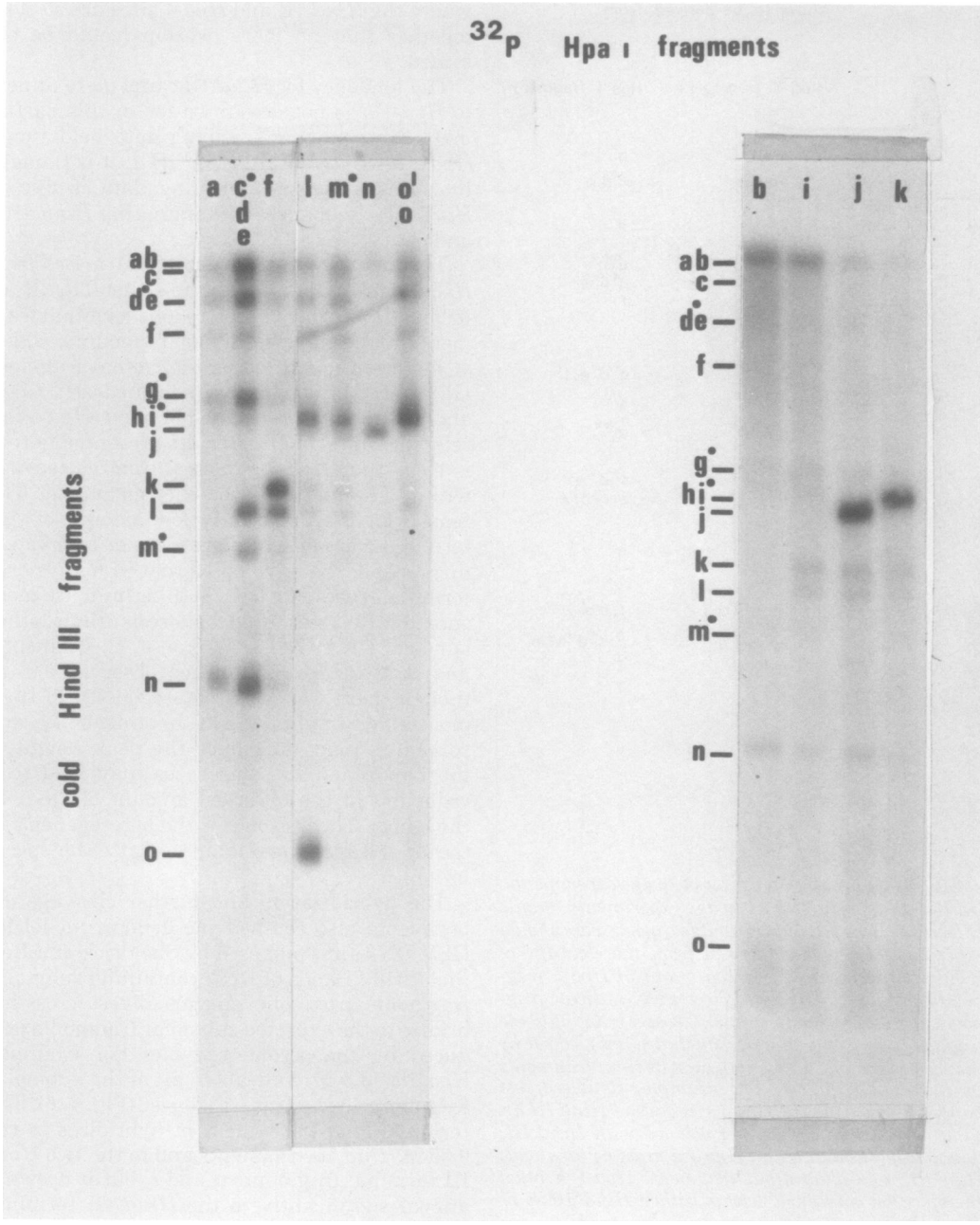

FIG. 4. *Hybridization of isolated ^{32}P-labeled Hpa-1 fragments to unlabeled Hind III fragments of HSV-1 DNA. The technique was that described previously (12, 15) and annealing of labeled DNA to unlabeled DNA on nitrocellulose membrane strips was determined by autoradiography. The positions of all of the unlabeled DNA bands on nitrocellulose membrane strips were located by annealing with fragmented, unfractionated ^{32}P-labeled HSV-1 DNA. Terminal fragments are indicated by the solid circle.*

firmed by Wadsworth et al. (13) may cause internal reassociation (in the unlabeled DNA) which might interfere with the reassociation reaction.

Analysis of *X. bad* digests. *X. bad* fragments of HSV-1 DNA can be separated into six bands by electrophoresis on 0.3% agarose (Fig. 1). Analysis of the mass distribution of the DNA in

COLD HPA-1 FRAGMENTS	³²P-LABELED HIND III FRAGMENTS: ab	c	de•	f	g•	hi•	j	k	l	m•	n	o	
a	+	+	+		+					+	++		a
b	+	+	+										b
c•de	++	++	++		++				++	++	++		c•de
f								++	++		(+)		f
g•h	+		+		+					+			g•h
i	+												i
j							++						j
k						++						+++	k
l			+			+							l
m•			+			+							m•
n							++						n
oo'			+			++							oo'
p			+										p

FIG. 5. *The hybridization of ³²P-labeled Hind III fragments to unlabeled Hpa-1 fragments. Solid circles (●) indicate terminal fragments. The amount of label in each band (above that level caused by contaminating sequences) was assessed by eye for each strip and allocated +, ++, or +++ in order of increasing intensity.*

COLD HIND III FRAGMENTS	³²P-LABELED HPA-1 FRAGMENTS: a	b	c•de	f	g•h	i	j	k	l	m•	n	oo'	p	q	r	s	
ab	+	++	+		++	++			+	+	+	+	+	+		+	ab
c	+		+		+				+	+		+	+			+	c
de•	++		+		+				++	++		++	+			+	de•
f	+		+		+				+	+		+					f
g•	+		+		++												g•
hi•	++		+					++	++	++		+++		(+)	+	+	hi•
j							++				++						j
k				++													k
l			+	+													l
m•	+		+	+	+												m•
n	+		+	+													n
o									++								o

FIG. 6. *The hybridization of ³²P-labeled Hpa-1 fragments to unlabeled Hind III fragments.*

those bands by the techniques described in a previous publication (1) give the mass percentage of the six bands *a, b, c, de, f, g* as 19, 11.2, 26, 27, 13, 3.2. The molecular weights of these fragments were estimated from slab gels and from the further analysis and mapping of *X. bad* fragments to be 34×10^6, 22×10^6, 21×10^6, 18×10^6, 15×10^6, and 6.5×10^{-6}, respectively. From these figures, and assuming a molecular weight of about 98×20^6 for HSV-1 DNA, the molarities for *a, b, c, de, f,* and *g* could be calculated to be 0.55, 0.51, 1.2, 1.46, 0.85, and 0.48. This suggests that *a, b, d,* or *e,* and *g* are 0.5 M fragments and that *c, d* or *e,* and *f* are molar fragments. As before, *d* was designated as the 0.5 M fragment, and *e* was designated as the molar fragment.

Analysis of *X. bad/Hind* III, and *X. bad/Hpa*-1 double digests (e.g., Fig. 1) clearly indicate that there are only four cleavage sites for *X. bad* in HSV-1 DNA. One site lies in *Hind* III *l* and *Hpa*-1 *e*, two in *Hind* III *a* (one each in *Hpa*-1 *b* and *i*), and the remaining site in *Hind* III *i* (and its inversion *Hind* III *f*) and in *Hpa*-1 *l*. These *X. bad* sites are shown in the partial map in Fig. 7. The two cleavage sites in *Hind* III *a* were confirmed by the further digestion of isolated *Hind* III *ab* with *X. bad*. Three further cleavage products were identified with molecular weights of 15×10^6, 8×10^6, and 2.8×10^6. The 15×10^6 fragments had the same mobility as *X. bad f.*

The four cleavage sites all lie in the L region of the genome and would give rise to seven fragments because of the inversion of the L region: an enzyme which cleaves only in the L region should produce two 0.5 M terminal fragments which contain the S sequences and two 0.5 M fragments from the L terminus. All other fragments should be molar. This fits very well with the cleavage profile and the estimates of molecular weights and molarities obtained for the *X. bad* fragments. *X. bad a* and *b* are the 0.5 M termini from the S region; *X. bad d* and *g* are the 0.5 M termini from L; and *X. bad c, e,* and *f* are the remaining internal molar fragments from L. This analysis of the *X. bad* cleavage pattern offers further confirmation of the partial map shown in Fig. 7.

Completion of the map. The position of the *X. bad* sites on the HSV-1 DNA map provides the necessary overlaps that allow completion of the map. ³²P-labeled *Hind* III fragments *k* and *o* and *Hpa*-1-labeled fragments *b, j,* and *k* were

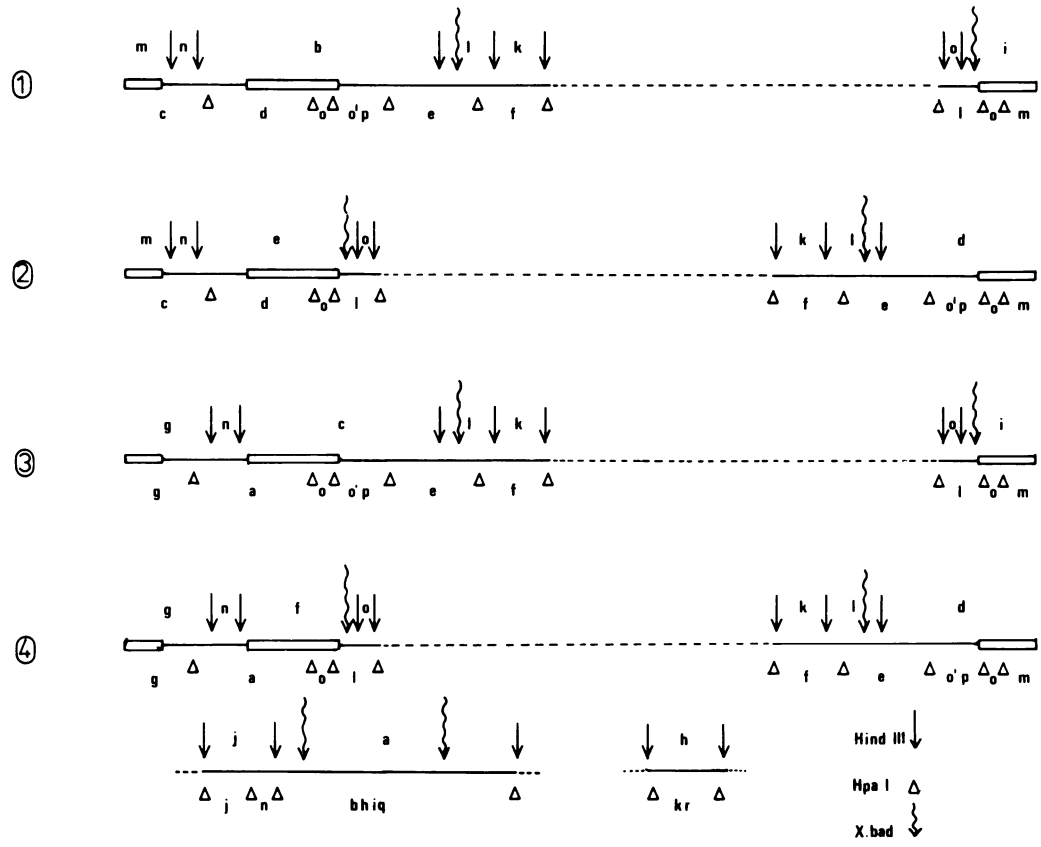

FIG. 7. *Partial map of Hind III and Hpa-1 fragments of HSV-1 DNA.*

annealed to unlabeled *X. bad* fragments using the DNA transfer or blot technique (12) as before (15). The results are summarized in Fig. 8. *Hpa*-1 *b* hybridized mainly to *X. bad f* and also to *d*. This confirmed the previous suggestion that *X. bad f* is contained within *Hind* III *a*. Hpa-1 *j* and *k* and *Hind* III *o* hybridized mainly to *X. bad c*, whereas *Hind* III *k* hybridized mainly to *X. bad de*. Since *X. bad d* is a terminal fragment from L, its sequences must also be contained in one larger 0.5 M fragment (*a* or *b*) from the S region. The hybridization of *Hind* III *k* mainly to *X. bad de* must therefore be to the unique fragment *e*. From the partial map shown in Fig. 7 it can be seen that *X. bad e* must lie adjacent to the *Hind* III *b/l* and *c/l* junction. Since *Hind* III *o* and *Hpa*-1 *k* both anneal to *X. bad c*, *Hind* III *h* must lie on the *Hind* III *o* side of the gap in the partial map shown in Fig. 7. Thus, *X. bad c* must lie in the region of the *Hind* III *h/o* junction. This leads to the following unequivocal order of *X. bad* fragments in the four arrangements of the genome shown in Fig. 7 and 10:

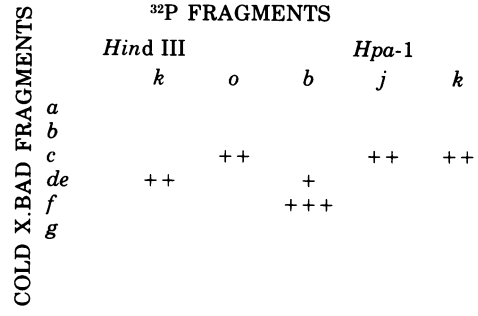

FIG. 8. *The hybridization of* ^{32}*P-labeled Hind III and Hpa-1 fragments to unlabeled X. bad fragments.*

(1) *a e f c g* (2) *b c f e d*
(3) *a e f c g* (4) *b c f e d*

Since only two arrangements are possible for L, there are only two possible *X. bad* maps.

Since Hpa-1 *j* and *k* both annealed to *X. bad c*, both must be adjacent to the *Hind* III *o* region in the partial map of Fig. 7. The only way these linkage groups can be arranged in the L region

is therefore (in the order for the *Hind* III fragments): *l k a j h o*.

Hind III *a* contains two cleavage sites for *X. bad*, which give rise to the three further cleavage products at 15×10^6, 8×10^6, and 2.8×10^6 daltons. *Hpa*-1 *b* and *i* each contain one of these *X. bad* sites. The only interior arrangement of *Hpa*-1 *b*, *h*, and *i* that allows the further cleavage products actually observed is:

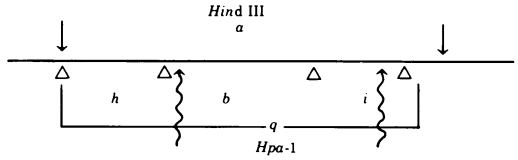

where ⇕ = *X. bad*; ↓ = *Hind* III, and △ = *Hpa*-1.

The results do not allow the location of *Hpa*-1 *q* within *Hind* III *a*. Since *Hpa*-1 *q* is small (1.7×10^6 daltons) this does not affect the relative order of *Hpa*-1 *b*, *h*, and *i* within *Hind* III *a*. (The hybridization of ^{32}P-labeled *Hpa*-1 *q* to unlabeled *X. bad* fragments should allow the unequivocal assignment of *q*.) The final orientation of the maps was obtained by hybridizing ^{32}P-labeled Hpa-1 fragments to unlabeled *X. bad*/*Hind* III double-digest fragments using the DNA transfer or blot technique (14). The results are shown in Fig. 9. *Hpa*-1 *i* hybridizes to two fragments, as expected from the small section of the map shown immediately above. *Hpa*-1 *n* hybridizes to the smaller of these two fragments and also to a higher-molecular-weight fragment. *Hpa*-1 *j* anneals exclusively to this larger fragment, which has a mobility the same as that of *Hind* III *j* (which is a limit fragment in the *X. bad*/*Hind* III double digest). This confirms the *Hpa*-1 map order in this region as:

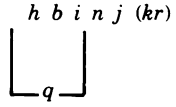

Taking all these results together, the complete cleavage fragment maps for *Hind* III, *Hpa*-1, and *X. bad* shown in Fig. 10 can be constructed. The results do not allow the final order of *Hpa*-1 *o* and *p*, of *Hpa*-1 *k* and *r*, or the final position of *Hpa*-1 *q* within *Hind* III *a* to be assigned. The hybridization results with *Hpa*-1 *s* did not give a unique location on the map. However, it is possible that *Hpa*-1 *s* is in fact two fragments. In this case, the hybridization data shown in Fig. 5 can be explained if one of the fragments, *Hpa*-1 *s*, lies in the *o'p* region of the map, and the other fragment, Hpa-1 *s'*, lies in the linkage group *kr* within *Hind* III *h*.

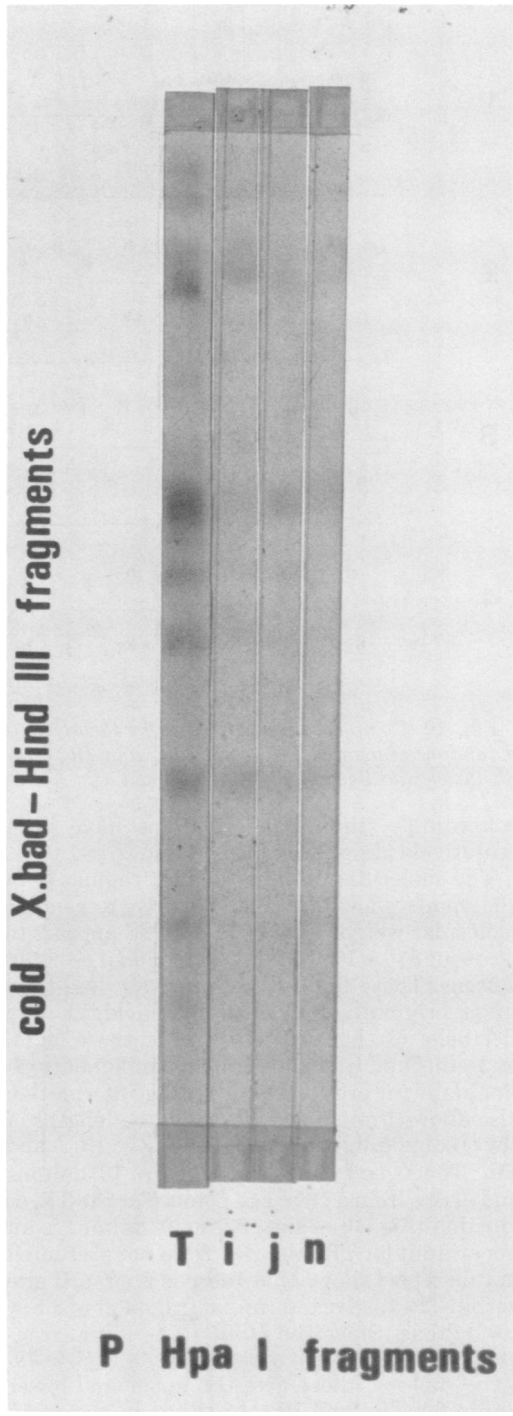

FIG. 9. *Hybridization of ^{32}P-labeled Hpa-1 fragments of HSV-1 DNA to unlabeled X. bad-Hind III double-digest fragments. T means the hybridization of fragmented, unfractionated ^{32}P-labeled HSV-1 DNA to cold fragments.*

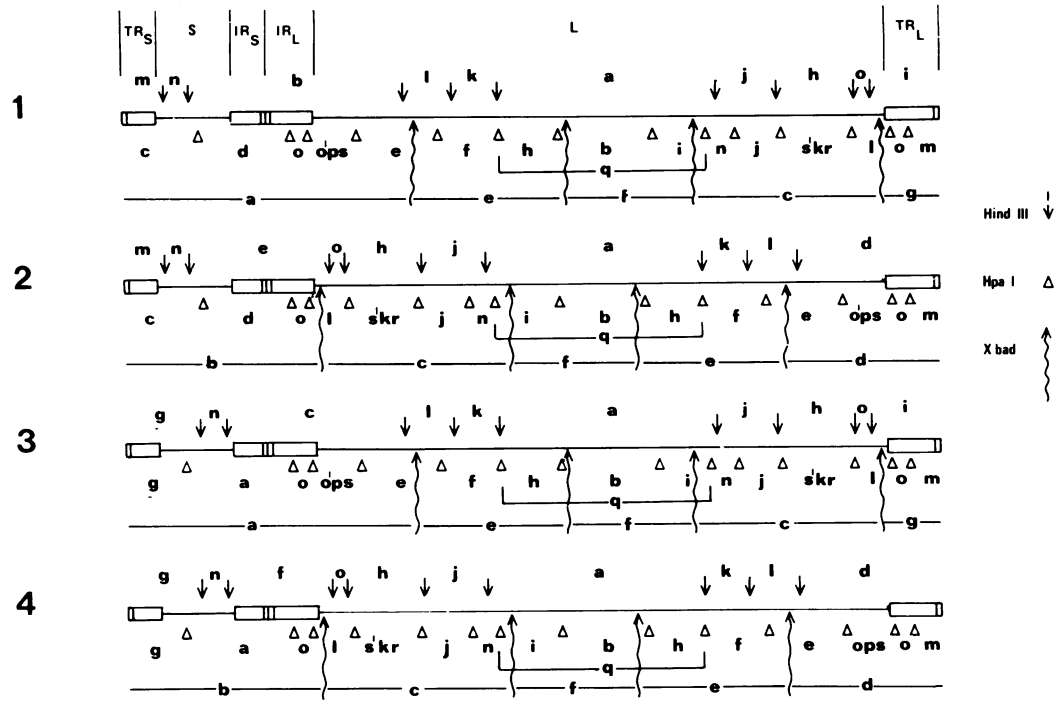

FIG. 10. *Complete physical maps for the Hind III, Hpa-1, and X. bad fragments of HSV-1 DNA. The redundant sequences TR_L, IR_L, TR_S, and IR_S and the unique sequences L and S, originally proposed by Sheldrick and Berthelot (10), are shown.*

Accordingly, these map positions have been tentatively assigned to *Hpa*-1 *s* and *Hpa*-1 *s'*.

The molecular weights of the fragments in the maps shown in Fig. 10 give a genome molecular weight total of 98×10^6. S appears to be about $8^{-9} \times 10^6$ daltons, and L about 68×10^6 daltons. These figures are somewhat less than those originally published by Sheldrick and Berthelot (3), but are very close to those found by Delius and Clements from partial denaturation data (in press). The mapping information also allows limits to be placed on the lengths of the redundant sequences TR_S/IR_S, IR_L, and TR_L. The *X. bad* end *g* is about 6.5×10^6 daltons and arises from a cleavage point near the TR_L/L junction (Fig. 10). Thus, 6.5×10^6 daltons is an upper limit for TR_L and IR_L. Data not presented in this report shows that there is an *Eco*RI site within TR_S to give a terminal fragment of 3.5×10^6 daltons. Since the *Hind* III terminal fragment *m*, arising from a cleavage site in S, is 4.5×10^6 daltons, these give the upper and lower limits for TR_S and IR_S. In the map shown in Fig. 10, TR_L/IR_L and TR_S/IR_S have been drawn as 6×10^6 daltons and 4×10^6 daltons, respectively. These estimates are very similar to the figures of 6 and 4% for TR_L/IR_L and TR_S/IR_S derived by Clements and Delius (in press) from their complete partial-denaturation maps of HSV-1 DNA. Since there is some indication (15) that the true terminal redundancy of 0.5×10^6 daltons (2, 3, 10) may be repeated in the internal inversions of TR_S and TR_L, this sequence has been indicated in the maps shown in Fig. 10 as a separate division within each redundant region.

The restriction enzyme maps of HSV-1 DNA for *Hind* III, *Hpa*-1, and *X. bad* shown in Fig. 10 should form the basis for further restriction endonuclease maps. Additional mapping work should also eliminate the remaining minor uncertainties in the *Hpa*-1 maps.

ACKNOWLEDGMENTS

This work was carried out at the Cold Spring Harbor Laboratory during temporary leave of absence from the Institute of Virology in Glasgow. I am grateful to J. Watson for making available the facilities at the Cold Spring Harbor Laboratory and to J. Sambrook for many helpful discussions. Janet Arrand and Rita Cortini provided invaluable assistance.

LITERATURE CITED

1. **Clements, J. B., R. Cortini, and N. M. Wilkie.** 1976. Analysis of herpesvirus DNA substructure by means of restriction endonucleases. J. Gen. Virol. 30:243-256.
2. **Grafstrom, R. H., J. C. Alwine, W. L. Steinhart, and C. W. Hill.** 1974. Terminal repetitions in herpes simplex

virus type 1 DNA. Cold Spring Harbor Symp. Quant. Biol. 39:679-681.

3. **Grafstrom, R. W., J. C. Alwine, W. L. Steinhart, C. W. Hill, and R. W. Hyman.** 1975. The terminal repetition of herpes simplex virus DNA. Virology 67:144-157.
4. **Hayward, G. S., N. Frenkel, and B. Roizman.** 1975. Anatomy of herpes simplex virus DNA: strain differences and heterogeneity in the location of restriction endonuclease cleavage sites. Proc. Natl. Acad. Sci. U.S.A. 72:1768-1772.
5. **Hayward, G. S., R. J. Jacob, S. C. Wadsworth, and B. Roizman.** 1975. Anatomy of herpes simplex virus DNA: evidence for four populations of molecules that differ in the relative orientations of their long and short components. Proc. Natl. Acad. Sci. U.S.A. 72:4243-4247.
6. **Hyman, R. W., S. Burke, and L. Kudler.** 1975. A nearby inverted repeat of the terminal sequence of herpes simplex virus DNA. Biochem. Biophys. Res. Commun. 68:609-615.
7. **Maniatas, T., A. Jeffrey, and D. G. Kleid.** 1975. Nucleotide sequences of the rightward operator of phage lambda. Proc. Natl. Acad. Sci. U.S.A. 72:1184-1188.
8. **Roizman, B., M. Kozak, R. W. Honess, and G. Hayward.** 1974. Regulation of herpesvirus macromolecular synthesis: evidence for multilevel regulation of herpes simplex 1 RNA and protein synthesis. Cold Spring Harbor Symp. Quant. Biol. 39:687-701.
9. **Sharpe, P. A., B. Sugden, and J. Sambrook.** 1975. Detection of two restriction endonuclease activities in *Haemophilus parainfluenzae* using analytical agarose-ethidium bromide electrophoresis. Biochemistry 12:3055.
10. **Sheldrick, P. and N. Berthelot.** 1974. Inverted repetitions in the chromosome of herpes simplex virus. Cold Spring Harbor Symp. Quant. Biol. 39:667-678.
11. **Skare, J., W. P. Summers, and W. C. Summers.** 1975. Structure and function of herpesvirus genomes. I. Comparison of five HSV-1 and two HSV-2 strains by cleavage of their DNA with *Eco*RI restriction endonuclease. J. Virol. 15:726-732.
12. **Southern, E. M.** 1975. Detection of specific sequences among DNA fragments separated by gel electrophoresis. J. Mol. Biol. 98:503-518.
13. **Wadsworth, S., G. S. Hayward, and B. Roizman.** 1976. Anatomy of herpes simplex DNA. V. Terminally repetitive sequences. J. Virol. 17:503-512.
14. **Wilkie, N. M., J. B. Clements, J. C. M. Macnab, and J. H. Subak-Sharpe.** 1974. The structure and biological properties of herpes simplex virus DNA. Cold Spring Harbor Symp. Quant. Biol. 39:657-666.
15. **Wilkie, N. M., and R. Cortini.** 1976. Sequence arrangement in herpes simplex type 1 DNA: identification of terminal fragments in restriction endonuclease digests and evidence for inversions in redundant and unique sequences. J. Virol. 20:211-221.